ACS APPLIED MATERIALS & INTERFACES

Research Article

www.acsami.org

Thermal Transformation of Carbon Hybrid Materials to Graphene Films

Rajanish N. Tiwari,*[,†] M. Ishihara,[†] Jitendra N. Tiwari,[‡] and Masamichi Yoshimura[†]

[†]Toyota Technological Institute, 2-12-1 Hisakata, Tampaku-ku, Nagoya 468-8511, Japan

[‡]Center for Superfunctional Materials, Department of Chemistry, Pohang University of Science and Technology, San 31, Hyojadong, Namgu, Pohang 790-784, Korea

Supporting Information

ABSTRACT: We demonstrate a simple approach to grow graphene films on polycrystalline nickel (Ni) foils, in which polycrystalline carbon hybrid materials (CHMs) were used in sandwich structures (molybdenum-CHMs-Ni-molybdenum) as a carbon source for graphene, and pressure was then applied to the sandwich. The CHMs were transformed into single as well as few layer graphene by a segregation−precipitation process. The applied pressure not only increased the density of the graphene films but also reduced the vaporization of dissociated carbon molecules of the CHMs. We have explored the possibility to grow graphene films in low vacuum (5×10^{-1} Pa) at relatively low temperatures (≤750 °C). The formation of the graphene films at 750 °C is simple and cost-effective and can be scaled up.

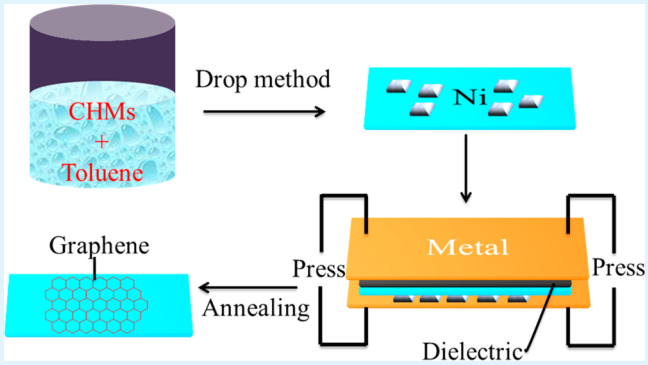

KEYWORDS: *carbon hybrid materials, sandwich structure, graphene*

INTRODUCTION

Graphene, a two-dimensional (2D) carbon atoms whose structure is based on one-atom-thick planar sheets of carbon atoms that are arranged in hexagonal lattices, was discovered by Geim et al. in 2004.[1] It has attracted huge scientific interest due to its excellent quantum electronic transport, bandgap opening, outstanding thermal conductivity and high mechanical strength with ultrathin geometry.[2−5] Exceptional properties of graphene makes extremely broad technological applications for instances composites, transparent conductive films, lithium-ion batteries, supercapacitors, organic photovoltaic cells, hydrogen storage, electron field emitters, field effect transistors, ultrasensitive sensors, and so on.[4−10] As we know, the most physical studies of graphene are carried out by the "scotch-tape" method, wherein a monolayer graphene formed from highly ordered pyrolytic graphite.[1,5] However, this technique clearly cannot be employed either for large-scale applications or to study numerous of the chemical and materials properties in detail due to small size and low yield. Therefore, in the past few years, many efforts have been devoted to developing several methods with new materials to grow graphene films; however, each method has its own advantages and disadvantages.

Several methods have been developed to produce graphene such as chemical method of graphene oxide has been promising route to achieve mass-production graphene.[11,12] However, the complicated and multistep process is to synthesize graphene by chemical routes such as oxidation, reduction, centrifugation in liquid phase along with chemical and structural defects. Epitaxial graphene has also been prepared by thermal decomposition of SiC under ultrahigh vacuum and high temperature (≤1100 °C).[13,14] Recently, chemical vapor deposition growth method is good technique to grow graphene at high temperatures on the various metal substrates.[4,5,10,15−17] Recently, Li et al. and Weatherup et al. have reported graphene films by CVD at low temperatures ≤700 °C.[18,19] However, well-sealed chambers and explosive gaseous raw carbon sources (methane or ethane) used in this process to get graphene. It is also possible to get graphene from sources other than gaseous hydrocarbons. Sun et al. has reported graphene formation from solid carbon sources at high temperatures (≤1000 °C).[20] The high-temperature graphene growth on Ni−Mo alloy by segregation−precipitation process has also been recently reported.[21] It is well-known that the high growth temperatures impose limitations on the choice of substrates. Therefore, it is indeed necessary to develop simple, easy and cost-effective approach to obtain defect free graphene films at low temperature for broad range of applications.

In this study, we describe a very unique and simple approach to synthesize graphene films onto polycrystalline metal substrate (Ni) at relatively low temperatures (≤750 °C). Our synthesis methodology is based on decomposition, diffusion, and precipitation. The applied pressure on the sandwich

Received: February 28, 2013
Accepted: June 18, 2013
Published: June 18, 2013

   dx.doi.org/10.1021/am401805u | ACS Appl. Mater. Interfaces 2013, 5, 6522−6526

structures improves contact area between metal (Ni) and carbon source (CHMs), more graphene films can be formed at relatively low temperatures. Annealing for a few minutes allows deposited carbon on the polycrystalline Ni foils to diffuse predominantly along grain boundaries to form a thin graphene film on the metal surface. This study proposes that graphene films in good scale that can be simply prepared by segregation–precipitation process are highly desirable for transparent conductor.

MATERIALS AND METHODS

The schematic of the preparation process is illustrated in Figure 1. The synthesis processes of the graphene films on Ni substrates are

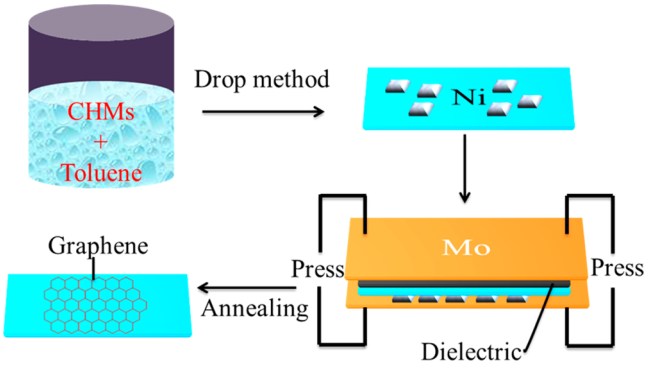

Figure 1. Schematic diagrams represent the graphene synthesis on Ni surface in four steps: (A) CHMs + toluene solution, (B) one drop of solution placed on Ni surface, (C) prepared five-layer sandwich structures (Mo/CHMs/Ni/dielectric/Mo), and (D) annealed sandwich structures to get graphene on the Ni surface.

described as follows: the polycrystalline Ni sheets with dimensions of 6 × 6 mm^2 were used as the substrates. The Ni substrates were ultrasonically cleaned with acetone for 10 min and then air blower was used to remove the any remaining particles from the Ni surface. Further, carbon hybrid materials (CHMs) (adamantane + fullerene in 1:1 ratio) were dissolved in toluene solvent and then magnet stirred for 1 h at room temperature. Prior to dissolve CHMs in toluene solvent, CHMs were first ground and mixed it completely. Further, one drop of solution (CHMs+ toluene) were only put on the Mo surface (here Mo is used as a support for Ni). We did not put CHMs on to Ni sheets. And then, the deposited CHMs on Mo (thickness; 200 μm) were covered by Ni (thickness; 10 μm) sheets. Further, we used dielectric material (SiO_2/Si surface) on the Ni surface (Mo/CHMs/Ni/dielectric). Finally, we used another Mo sheet (thickness; 200 μm) on the structures (Mo/CHMs/Ni/dielectric/Mo) and manually applied pressure on the structures, as shown in Figure 1. After applied pressure on the sandwich structures, the synthesis process was carried out under low vacuum such as 5 × 10^{-1} Pa. We used (ULVAC-RIKO MILA-5000) annealing lamp to anneal the sandwich structures at 750 °C for 10 min. To know the role of pressure, we prepared without created pressure (without screw) on sandwich structure (Mo/NC/Ni/Dielectric/Mo) and treated with the same experimental conditions.

The surface morphology of the sample was examined using field-emission scanning electron microscope (FESEM, Hitachi 6700), optical microscopy, high-resolution transmission electron microscopy (HRTEM) and scanning tunneling microscopy (Nanosurf Easyscan2 STM). Raman spectroscopy was performed using a RENISHAW system with a diode laser (wavelength = 532 nm), which could be focused to a diameter of 1 μm for micro mode operation.

RESULTS AND DISCUSSION

The schematic of the preparation process of graphene is illustrated in Figure 1. The CHMs were deposited on metal substrates by spin coating is shown in Figure 1. The FESEM image of deposited CHMs on Si is shown in Figure 2A. It

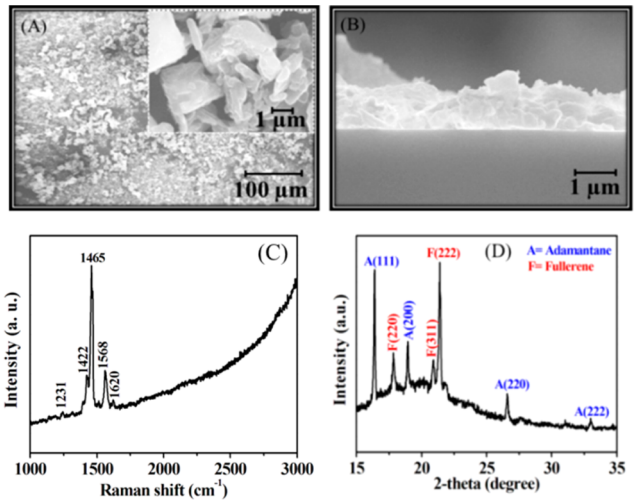

Figure 2. (A) Top-view; inset, high-magnification SEM image; (B) side-view; inset, high-magnification SEM image; (C) Raman spectrum; and (D) XRD pattern of CHMs.

seems the crystalline CHMs were deposited on the Si surface by spin coating. From the FESEM top-view, it is clear that CHMs were uniformly distributed on the surface by spin-coating. However, a high-magnified FESEM image in Figure 2A shows the particles sizes of CHMs were varied from 1 to 4 μm. As we know the sublimation property of adamantane is very high. Therefore, we mixed both carbon materials in same (1:1) ratio of CHMs and to get single layer graphene at partially low temperatures. As we know, the solubility of materials depends on (i) solvent–solvent, (ii) solvent–solute, and (iii) solute–solute interactions. Therefore, we noticed microsized cubic crystalline particles as well as few rod-like crystal structures have been formed in toluene solvent. The crystalline structure/morphology depends on the crystal structure of materials (adamantane has cubic while fullerene behaves as a hexagonal crystal structure). The cross-sectional FESEM in Figure 2B shows that the ∼900 nm CHMs were deposited on the Si substrate. Further, the deposited CHMs were characterized by Raman spectroscopy. The intense Raman peaks in the range of 1000–3000 cm^{-1} is shown in Figure 2C. We noticed multi Raman peaks at 1231, 1422, 1465, 1568, and 1620 cm^{-1}, as shown in Figure 2C. The multi Raman peaks correspond to both (adamantane + fullerene) carbon materials. The multi Raman peaks show the presence of different kind of CH/CH2 wag, twist and scissors modes. In addition, we used XRD to evaluate the CHMs on Si surface at ambient temperature. We observed multi peaks in XRD pattern as shown in Figure 2D. The XRD pattern in Figure 2D shows that the diffraction peaks at 2θ = 16.3, 17.3, 18.75, 20.76, 21.74, 26.75, and 33.0 correspond to the CHMs (adamantane + fullerene). The diffraction 2θ peaks at 16.3, 18.75, 26.75, and 33.0 correspond to the interplanar spacings of adamantane {111}, {200}, {220}, and {222} respectively while other 2θ peaks 17.3, 20.76, 21.74 correspond to fullerene {220}, {311}, and {222}, respectively, indicating that polycrystalline CHMs were deposited on the

dx.doi.org/10.1021/am401805u | ACS Appl. Mater. Interfaces 2013, 5, 6522–6526

surface.[22−27] It is also clear that the significant amount of CHMs molecules has only survived and toluene molecules either completely desorbed or presented in insignificant amount on the surface. Therefore, we did not notice any peak of toluene in Raman spectrum, as shown in Figure 2C. Therefore, we can conclude that polycrystalline CHMs were uniformly distributed on surface. After successfully deposited CHMs crystals as shown in Figure 2, we prepare sandwich structures and then manually applied pressure on the structures. We annealed the sandwich structures at various temperatures (600 to 750 °C) for 10 min. However, we did not observe single-layer graphene ≤700 °C (not shown here), whereas at ≥700 °C in 10 min annealing, we noticed single-layer graphene.

Further, the optical image contrast as well as Raman map shows the presence of number of graphene layers. As we know, Raman spectroscopy is a standard technique to characterize the chemical states of the bonds in carbon materials such as graphene, diamond, carbon nanotubes, diamond-like carbons, carbon nanowalls and so on.[28,29] Therefore, several researchers have used Raman spectra to characterize and quality control of mono- as well as multilayer of graphene film. The graphene shows D, G, and 2D peaks around 1350, 1580, and 2700 cm^{-1} respectively due to the change in electron bands. The D band appears due to the presence of disorder in atomic arrangement or edge effect of graphene, ripples and charge puddles while G band is associated to the doubly degenerated E2g phonon mode at the Brillouin zone center.[30] The graphene 2D peak is at almost double the frequency of the D band and originates from second order Raman scattering process. The Raman map image was used to know the structural morphology of graphene layers. The prepared sandwich structures in which CHMs were used as a carbon source were annealed at 750 °C for 10 min, found that CHMs (Figure 2C) were transformed into graphene on metal surface (The D, G, and 2D peaks appeared after annealing of CHMs) as shown in Figure 3. The typical Raman

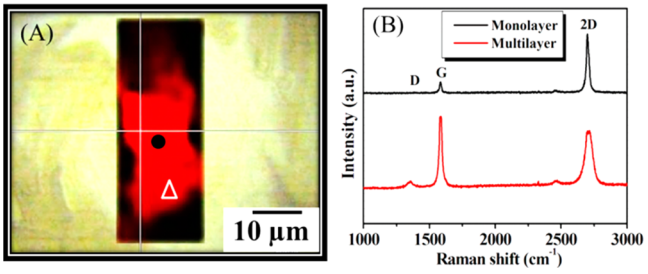

Figure 3. (A) Raman map image and (B) corresponding Raman spectra of graphene films.

map region in optical image is shown in Figure 3A. The red contrast in optical image shows the graphene formation on Ni surface. The Raman spectrum (black line) taken from bright red contrast image and is marked with contrasting black circle is shown in Figure 3B. We noticed the intensity ratio of I_{2D}/I_G is around ∼4.5 and full width and half maxima (fwhm) ∼23.4 cm^{-1}. The high intensity ratio of I_{2D}/I_G with low fwhm as shown in Figure 3B is a typical characteristic of single layer graphene. The absence of D peak shows that high quality single-layer graphene (defect free) is formed on the metal surface. However, the Raman spectrum (red line) from dark contrast (marked with triangle) in mapped region (Figure 3A) is shown in Figure 3B. We found low intensity ratio of I_{2D}/I_G is around ∼0.73 and fwhm ∼65.7 cm^{-1} shows the presence of multilayer graphene. The broad 2D peak indicating that multilayer graphene film has been formed after cool down. Probably, the broad 2D with small D peaks also indicates either the minimal interaction between the carbon−carbon or carbon−metal surface, therefore, small D peak appeared in the Raman spectra as shown in Figure 3 (red line). The clear mechanism for this phenomenon is not well understood and is currently under investigation. The D band originated in defects or disordered carbon is relatively strong in multilayer graphene (red line) than single layer graphene (black line). It is clearly represents the formation of inhomogeneous graphene films with different layer numbers including single as well as multilayer graphene in 10 min annealing at 750 °C. Here, we noticed the domain size of high quality single layer graphene is around ∼12 μm as shown in Figure 3A. The thin Ni foils (10 μm) usually bend under their own weight and can be torn easily during process. Therefore, these (bend or torn of metal foils) are not only responsible for defects, damage and impurities onto graphene structure but also increase the roughness of metal foils/films. Therefore, we used a clean, mirror-polished SiO_2/Si (dielectric) substrate over Ni foil (Mo/CHMs)/Ni/dielectric/Mo) to reduce these problems as well as improve the flatness of metal foils/films. We also expected that graphene will not only form on the metal (Ni) surface but also on dielectric materials (SiO_2/Si) which is used on the top of metal substrates (Mo/CHMs)/Ni/dielectric materials/Mo) in sandwich structures. However, we only observed amorphous carbon (D and G band) on SiO_2/Si surface, as shown in Figure 4. Images A and B in Figure 4 show

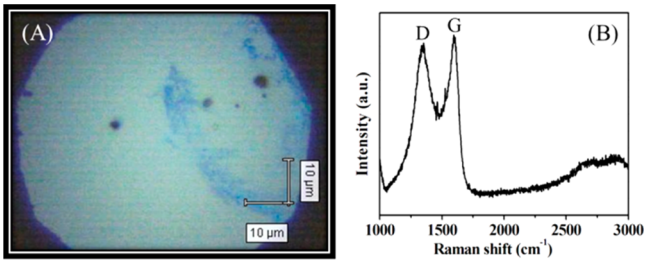

Figure 4. (A) Optical image and (B) Raman spectrum from dielectric surface (SiO_2/Si) after annealing of CHMs at 750 °C for 10 min.

the optical image of amorphous carbon formed on SiO_2/Si surface after annealing of CHMs at 750 °C for 10 min. We strongly conclude this technique offers the good reproducibility and produce graphene directly on metal substrate, as shown in Figure S1 in the Supporting Information. It is well-known that the formation of Ni−C interface (metastable Ni_3C) phase helps the diffusion and precipitation of carbon out of Ni. As we know, the graphene precipitation occurs more uniformly from limited sites when the appropriate amount of carbon is transported into metal surface. We observe that the carbon concentration is essential for the uniform single-layer graphene growth on Ni surface; however, higher carbon concentrations and rich grain boundaries (carbon preferentially precipitates out at the grain boundaries of polycrystalline Ni) easily give multilayer graphene, as shown in Figure 5. The optical image in Figure 5A shows dark contrast (marked with arrow) near the grain boundaries, give few layer graphene (Figure 5B) due to heterogeneous nucleation, whereas bright contrast shows single-layer graphene. Thus, uniform and controlled graphitization as well as low density of grain boundaries is most

dx.doi.org/10.1021/am401805u | ACS Appl. Mater. Interfaces 2013, 5, 6522−6526

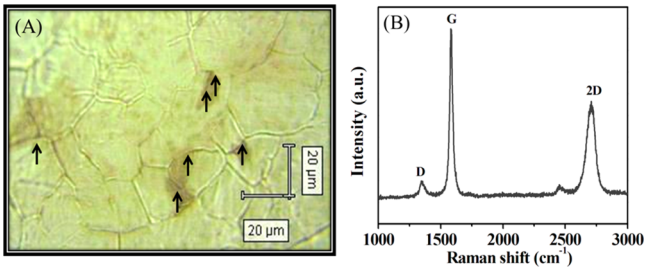

Figure 5. (A) Optical image and (B) Raman spectrum of multilayer layer graphene (arrows show the grain boundaries that give few-layer graphene).

important to get uniform single-layer graphene on metal surface.

To know the effect of pressure, we prepared a sandwich structures (without pressure) and then annealed it under exactly the same experimental conditions. In this case, we did not notice single layer graphene, however, few layer graphene were present on the metal surface, as shown in Figure 6.

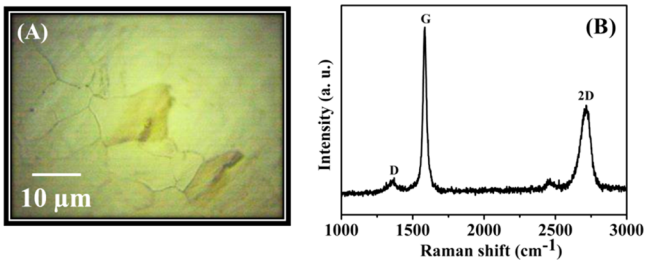

Figure 6. (A) Optical image and (B) Raman spectrum after annealing of sandwich structure (without pressure) at 750 °C for 10 min.

Probably, most of the carbon atoms from CHMs were pumped out at 750 °C in 10 min annealing time and only multilayer graphene/graphite formed in very few regions. Furthermore, the synthesized graphene films were characterized by STM at room temperature. In the measurements, cut Pt/Ir tip was used was used to obtain the STM topographs, as shown in Figure 7.

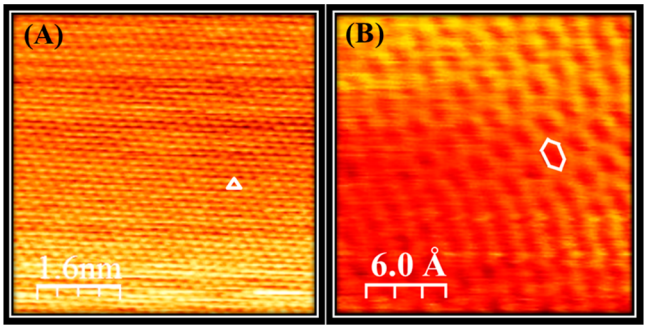

Figure 7. STM image of (A) multilayer and (B) single-layer graphene films on Ni surface after 10 annealing of CHMs at 750 °C.

The bias was set at a 0.15 V sample potential, and a tunneling current of 0.7 nA was chosen for single layer graphene. The STM image in Figure 7A shows the 3-fold symmetry characteristics of the surface of multilayer graphene/bulk graphite crystal. The graphene layers A and B stacked together and formed multilayer graphene films (3-fold symmetry) on the metal surface at 750 °C. However, the STM topographic image in Figure 7B shows the hexagonally symmetric honeycomb structure expected for an ideal, unperturbed graphene crystal has been formed at 750 °C for 10 min. It also confirmed that single as well as multilayer graphene films have been together formed on the metal surface. This is consistent with our optical images and Raman results. Furthermore, to know the quality of synthesized graphene films on metal surface at 750 °C, we transferred graphene on SiO_2(300 nm)/Si.[7] The optical image of transferred graphene is shown in Figure 8. The transferred

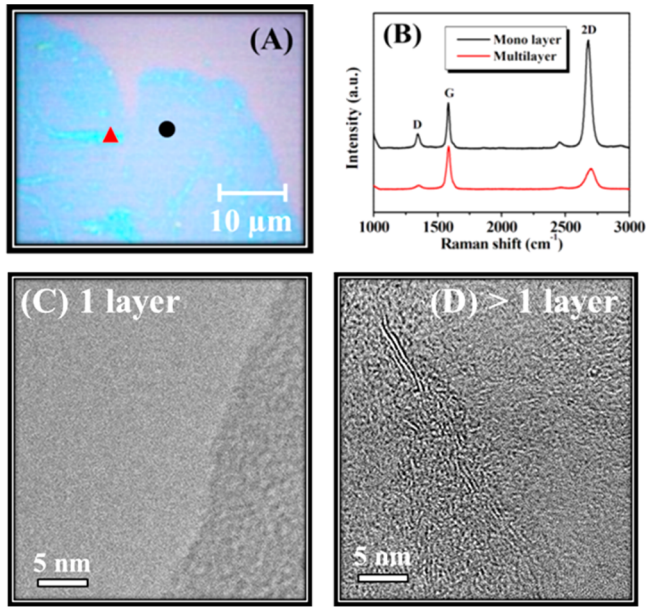

Figure 8. (A) Optical image of transferred graphene on SiO_2(300 nm)/Si, (B) corresponding Raman spectra of graphene, (C) HRTEM images of single- and (D) multilayer graphene film at 750 °C for 10 min annealing time.

graphene on the SiO_2/Si shows a uniform film, indicating the transfer was done without deteriorating the graphene film due to a protecting polymethyl methacrylate (PMMA) layer. We investigated the quality of the graphene after etching of metal by Raman spectroscopy, as shown in Figure 8B. We observed the relative intensity I_{2D}/I_G is around 2 with low fwhm (24.7 cm^{-1}) of transferred graphene. The low fwhm and the high intensity ratio show the high quality with good crystallinity of monolayer graphene has been formed on metal surface. This is the typical characteristics of the formation of single layer graphene.[1−5] The D peak as shown in Figure 8B was little higher than that measured after the transferred graphene, which signifies the possibility of graphene little damage during transfer process. Probably, the etching solution (0.5 M $FeCl_3$ aqueous solution) may damage the graphene film. In case of metal, carbon has higher affinity for metal substrate, therefore, the other prospect to form defects into the graphene structure is may be the dissolution of the Ni film may give dangling bonds in the graphene sheet, which reduces the domain size of the graphene and increases the D band intensity.[15] The study of interaction between graphene and the polycrystalline Ni foils and also for reduction of the D band intensity is still underway. The Raman spectrum (red line in Figure 8 (B)) taken from triangle marked region (Figure 8A shows the formation of multilayer graphene film. In addition, the structural morphology of the graphene sheets synthesized from CHMs at 750 °C for 10 min, were characterized by HRTEM. Images C and D

dx.doi.org/10.1021/am401805u | ACS Appl. Mater. Interfaces 2013, 5, 6522−6526

inFigure 8 show the HRTEM images of the obtained graphene with different number of layers. The observation of well-defined graphene edges by HRTEM provides an accurate way to measure the number of layers. Figure 8 (C) gives the evidence of single layer, whereas Figure 8D shows the multilayer graphene. We can strongly conclude that the single as well as multilayer graphene together formed at 750 °C in 10 min. The final thickness of the carbon layers depend on the amount of dissolved carbon into nickel by decomposition and diffusion process and then precipitation occurs on the metal surface. Therefore, we may control the graphene formation by controlling the parameters such as amount of carbon materials, applied pressure, temperature, cooling rate, and metal thickness. We also noticed the heavily grain boundaries supports to the formation of multilayer and smooth surface (less grain boundaries) assists to formation of uniform single layer graphene. Therefore, it is also very important to improve not only the nickel quality but also surface roughness.

CONCLUSIONS

In summary, we have developed a cost-effective, scalable, and sustainable process to fabricate high-quality graphene films from CHMs. We achieved single as well as few layers of graphene on metal substrate at 750 °C for 10 min. The applied pressure on the sandwich structures reduces the desorption properties of dissociated carbon molecules along with enhanced the graphene product at relatively low temperature in low vacuum. The proposed sandwich structures method and low-temperature growth method adopting solid carbon sources might have a simple, nontoxic, and economic way to get graphene. Moreover, this technique offers the good reproducibility and produce good quality graphene directly on metal substrate. The synthesized graphene holds promise not only for elegant scientific experiments but also for novel electronic devices and sensors.

ASSOCIATED CONTENT

Supporting Information

Additional figures (PDF). This material is available free of charge via the Internet at http://pubs.acs.org.

AUTHOR INFORMATION

Corresponding Author

*E-mail: rajanisht@gmail.com Tel: +81-52-809-1852; Fax: +81-52-809-1851.

Notes

The authors declare no competing financial interest.

ACKNOWLEDGMENTS

This study was supported in part by a grant of Support Program for Forming Strategic Research Infrastructure for Private Universities and KAKENHI (23651098) from Ministry of Education, Culture, Sport, Science and Technology, Japan (MEXT).

REFERENCES

(1) Novoselov, K. S.; Geim, A. K.; Morozov, S. V.; Jiang, D.; Zhang, Y.; Dubonos, S. V.; Grigorieva, I. V.; Firsov, A. A. *Science* **2004**, *306*, 666.
(2) Tiwari, R. N.; Ishihara, M.; Tiwari, J. N.; Yoshimura, M. *Polym. Chem.* **2012**, *3*, 2712.
(3) Zhang, Y.; Mori, T.; Niu, L.; Ye, J. *Energy Environ. Sci.* **2011**, *4*, 4517.
(4) Peng, Z.; Yan, Z.; Sun, Z.; Tour, J. M. *ACS Nano* **2011**, *5*, 8241.
(5) Singh, V.; Joung, D.; Zhai, L.; Das, S.; Khondaker, S. I.; Seal, S. *Progress in Mater. Sci.* **2011**, *56*, 1178.
(6) Li, Z.; Zhu, H.; Xie, D.; Wang, K.; Cao, A.; Wei, J.; Li, X.; Fan, L.; Wu, D. *Chem. Commun.* **2011**, *47*, 3520.
(7) Kahng, Y. H.; Lee, S.; Choe, M.; Jo, G.; Park, W.; Yoon, J.; Hong, W. K.; Cho, C. H.; Lee, B. H.; Lee, T. *Nanotechnology* **2011**, *22*, 045706.
(8) Joshi, R. K.; Gomez, H.; Alvi, F.; Kumar, A. *J. Phys. Chem. C* **2010**, *114*, 6610.
(9) Alwarappan, S.; Joshi, R. K.; Ram, M. K.; Kumar, A. *Appl. Phys. Lett.* **2010**, *96*, 263702.
(10) Shao, Y.; Wang, J.; Wu, H.; Liu, J.; Aksay, I. A.; Lin, Y. *Electroanalysis* **2010**, *22*, 1027.
(11) Wei, Z.; Wang, D.; Kim, S.; Kim, S. Y.; Hu, Y.; Yakes, M. K.; Laracuente, A. R.; Dai, Z.; Marder, S. R.; Berger, C.; King, W. P.; Heer, W. A.; Sheehan, P. E.; Riedo, E. *Science* **2010**, *328*, 1373.
(12) Cheng, M.; Yang, R.; Zhang, L.; Shi, Z.; Yang, W.; Wang, D.; Xie, G.; Shi, D.; Zhang, G. *Carbon* **2012**, *50*, 2581.
(13) Berger, C.; Song, Z.; Li, X.; Wu, X.; Brown, N.; Naud, C.; Mayou, D.; Li, T.; Hass, J.; Marchenkov, A. N.; Conrad, E. H.; First, P. N.; Heer, W. A. *Science* **2006**, *312*, 1191.
(14) Emtsev, K. V.; Bostwick, A.; Horn, K.; Jobst, J.; Kellogg, G. L.; Ley, L.; McChesney, J. L.; Ohta, T.; Reshanov, S. A.; Röhrl, J.; Rotenberg, E.; Schmid, A. K.; Waldmann, D.; Weber, H. B.; Thomas Seyller, T. *Nat. Mater.* **2009**, *8*, 203.
(15) Ago, H.; Ito, Y.; Mizuta, N.; Yoshida, K.; Hu, B.; Orofeo, C. M.; Tsuji, M.; Ikeda, K. I.; Mizuno, S. *ACS Nano* **2010**, *4*, 7407.
(16) Li, X.; Cai, W.; An, J.; Kim, S.; Nah, J.; Yang, D.; Piner, R.; Velamakanni, A.; Jung, I.; Tutuc, E.; Banerjee, S. K.; Colombo, L.; Ruoff, R. S. *Science* **2009**, *324*, 1312.
(17) Gao, L.; Ren, W.; Zhao, J.; Ma, L. P.; Chen, Z.; Cheng, H. M. *Appl. Phys. Lett.* **2010**, *97*, 183109.
(18) Li, Z.; Wu, P.; Wang, C.; Fan, X.; Zhang, W.; Zhai, X.; Zeng, C.; Li, Z.; Yang, J.; Hou, J. *ACS Nano* **2011**, *5*, 3385.
(19) Weatherup, R. S.; Dlubak, B.; Hofmann, S. *ACS Nano* **2012**, *6*, 9996.
(20) Sun, Z.; Yan, Z.; Yao, J.; Beitler, E.; Zhu, Y.; Tour, J. M. *Nature* **2010**, *468*, 549.
(21) Dai, B.; Fu, L.; Zou, Z.; Wang, M.; Xu, H.; Wang, S.; Liu, Z. *Nat. Commun.* **2011**, *2*, 522.
(22) Tiwari, R. N.; Chang, L. *J. Appl. Phys.* **2010**, *107*, 103305.
(23) Ginzburg, B. M.; Tuichiev, S.; Tabarov, S. K.; A. A. Shepelevski, A. A.; L. A. Shibaev, L. A. *Tech. Phys.* **2005**, *50*, 1458.
(24) Tiwari, R. N.; Ishihara, M.; Tiwari, J. N.; Yoshimura, M. *J. Mater. Chem.* **2012**, *22*, 15031.
(25) Tiwari, R. N.; Tiwari, J. N.; Chang, L. *Chem. Eng. J.* **2010**, *158*, 641.
(26) Meng, Z. D.; Zhu, L.; Choi, J. G.; Park, C. Y.; Oh, W. C. *Nanoscale Res. Lett.* **2011**, *6*, 459.
(27) Tiwari, R. N.; Ishihara, M.; Tiwari, J. N.; Yoshimura, M. *Chem. Commun.* **2012**, *48*, 3003.
(28) Ni, Z. H.; Fan, H. M.; Feng, Y. P.; Shen, Z. X.; Yang, B. J.; Wu, Y. H. *J. Chem. Phys.* **2006**, *124*, 204703.
(29) Tiwari, R. N.; Tiwari, J. N.; Chang, L.; Yoshimura, M. *J. Phys. Chem. C* **2011**, *115*, 16063.
(30) Ferrari, A. C.; Meyer, J. C.; Scardaci, V.; Casiraghi, C.; Lazzeri, M.; Mauri, F.; Piscanec, S.; Jiang, D.; Novoselov, K. S.; Roth, S.; Geim, A. K. *Phys. Rev. Lett.* **2006**, *97*, 187401.